Constructing 3D Diffusion Tensor Imaging using DICOM Files Directly and Linear Interpolation

2021 International Seminar on Machine Learning, Optimization, and Data Science (ISMODE) | 978-1-6654-0544-7/22/$31.00 ©2022 IEEE | DOI: 10.1109/ISMODE53584.2022.9742972

Maurendra Retawan Waluyo
Department of Informatics
Institut Teknologi Sepuluh Nopember
Surabaya, Indonesia
mrendra25@gmail.com

Salsabiil Hasanah
Department of Informatics
Institut Teknologi Sepuluh Nopember
Surabaya, Indonesia
salsabiilhasanah5@gmail.com

Aziz Fajar
Department of Informatics
Institut Teknologi Sepuluh Nopember
Surabaya, Indonesia
azizfajar519@gmail.com

Riyanarto Sarno
Department of Informatics
Institut Teknologi Sepuluh Nopember
Surabaya, Indonesia
riyanarto@if.its.ac.id

Chastine Fatichah
Department of Informatics
Institut Teknologi Sepuluh Nopember
Surabaya, Indonesia
chastine@if.its.ac.id

Sri Andreani Utomo
Department of Radiology
Dr Soetomo General Hospital
Department of Radiology
Faculty of Medicine
Universitas Airlangga
Surabaya,Indonesia
sriandreaniutomo@gmail.com

Kelly Rossa Sungkono
Department of Informatics
Institut Teknologi Sepuluh Nopember
Surabaya, Indonesia
kelly@its.ac.id

Francisca Notopuro
Department of Radiology
National Hospital
Surabaya, Indonesia
franciscanotopuro@gmail.com

***Abstract*— Diffusion Tensor Imaging (DTI) is a process to determine the diffusion of water molecules in the body, especially in the brain. This process can be used to extract the neural fibers in the brain. In this study, we proposed an approach for constructing three-dimensional (3D) DTI using Digital Imaging and Communications in Medicine (DICOM) files directly and linear interpolation to improve the quality of neural fibers extraction results. Based on the experimental results, the average amounts of neural fibers generated using our approach are 155534 fibers. Meanwhile, the use of Neuroimaging Informatics Technology Initiative (NIfTI) data that was widely used in recent studies resulted in an average of 117028 fibers. So that there was an increase of 38606 fibers or about 32.9%. In addition, the metadata of the DICOM file is still stored properly and can be used for further 3D image processing. The greater amounts of fibers indicate that the more complete the fibers produced and can be more helpful for doctors to check for abnormalities that may exist.**

Keywords— Diffusion Tensor Imaging, Fiber Tracking, DICOM, NIfTI, Linear Interpolation

I. INTRODUCTION

Techniques in the medical world used to find out the inside of the human body in detail are called Magnetic Resonance Imaging (MRI) [1]. The image results from these techniques can be in Digital Imaging and Communications in Medicine (DICOM) files. In the MRI technique, the observation process is carried out on each slice of the body part with a predetermined distance [2]. There are many fields of research that can be done using the results of this MRI process, the example that is mostly done is segmentation to get certain brain anatomy [3–5]. Another results of MRI data processing is DTI. DTI is a process that can be further developed to perform neural fibers extraction by adding fractional anisotropy (FA) and fiber tracking methods. The results of this neural network extraction are useful to be able to see abnormalities in the neural fibers of the human brain.

The results of the neural fibers extraction process are utilized by several studies for further medical analysis. As in some studies [3–6] discussing the analysis of DTI results in certain types of abnormalities in the human brain. Some abnormalities in the brain have different tendencies of neural fibers structure. The use of DTI can also be done to compare neural fibers structures in certain age groups.

Currently, the implementation of neural fibers extraction using DTI tends to use NIfTI data types. This is evidenced in several recent studies [7–13] that use NIfTI data as input for the DTI process. NIfTI data is a type of data obtained from the results of DICOM file conversion [17]. This type of data has a simpler structure than DICOM files [15]. Many studies use NIfTI files due to the simplicity of their structure. However, in NIfTI files a lot of metadata is removed from DICOM files. Thus, NIfTI files will not be able to be converted back into DICOM file forms with their original metadata due to the amounts of metadata that are omitted. The image resolution on NIfTI files is also less good than indirect DICOM files.

Based on the problems mentioned, we propose an approach for constructing 3D diffusion tensor imaging using DICOM files directly to maintain existing metadata and improve the quality of neural fibers extraction results. We also added a linear interpolation method to improve the shape of 3D diffusion tensor imaging that has pixel spacing too large that affects the results of 3D images. The direct use of DICOM data and the addition of linear interpolation method are expected to improve neural fibers extraction results and maintain the metadata stored in them. Metadata information that is still stored properly can be used in the next 3D image processing.

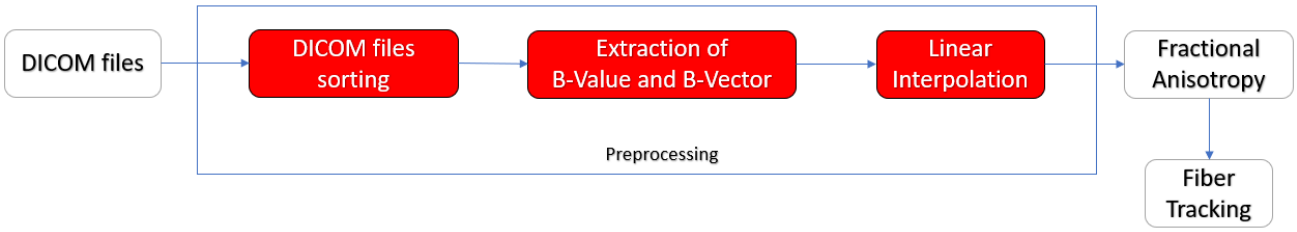

Fig. 1. Proposed method

This paper is structured into some parts. Sections 2 describes literature review. Then, the research methodology is in Section 3. The experimental results and discussion are presented in Section 4. Finally, Section 5 draws conclusions and the following research.

II. Literature Review

Many types of research on DTI have been done before. DTI can be used for several things that are beneficial to the world of health. Such as the use of DTI for the analysis of several types of diseases carried out by several studies [15, 16], to the use of DTI to assist in planning surgical procedures [17–19].

In previous studies, DTI processing is often done by converting the DICOM data to NIfTI data form. In 2021, [23] conducted a study using DTI to analyze classifying Alzheimer's Disease (AD). It proves that DTI is good for identifying AD. Another study on AD was conducted by Pan et al. [15] in 2021. This study proposes a new approach using decoupling generative adversarial network (DecGAN) to detect abnormal neural circuits for AD. Both studies regarding the use of DTI in the context of AD used the DICOM files that have been converted to NIfTI form first.

Besides the use of DTI for the context of AD, the use of DTI is also often used for the analysis of several other diseases for health needs. One example was the study [10] which used DTI for analysis of changes in the MRI microstructure of the parkinsonian peripheral olfactory system and in particular the olfactory tract. In this study, DICOM data was converted to NIfTI using the free dcm2nii software. Xia et al. [16] conducted a study in the context of diabetes to explore the relationship between DTI parameters and electrophysiological parameters. The preprocessing process was carried out by converting DICOM data to NIfTI form using MRIConvert.

The use of NIfTI data that is often done in several previous studies was carried out because NIfTI data has a simpler structure than DICOM data. This NIfTI file is actually obtained from the converting DICOM file [17]. The use of NIfTI input is widely used for processing input from DTI because the file size is smaller so that the processing time is faster [24]. However, this process of converting DICOM files to NIfTI may cause some of their metadata information to be lost. Therefore, the use of DICOM files can be used instead of NIfTI files. In addition, there is much open-source software that can help the conversion process into NIfTI so that we can directly get data in the form of 3D images.

III. Methods

Several steps are performed to extract neural fibers in 3D form. These steps consist of preprocessing, fractional anisotropy, and fiber tracking. The steps performed in this study are shown in Fig. 1. Our proposed method is given a red color in the background.

A. DICOM File Sorting

The existing DICOM file consists of a collection of images in random order. These files must be sorted first in the order in which they should be sliced. The sorting process is done by reading the instance number metadata in the header of each DICOM file. The Instance Number metadata is obtained based on the DICOM tag number (0020, 0013). The instance number metadata indicates the position of the file that should be based on the existing direction. One example is when we read the header of a DICOM file named Z21. The metadata instance number in the header of the file shows the number 410. Therefore, based on the instance number value, we must put this file in the order of 410 of the total files. This is done continuously on the entire DICOM file.

When the whole file has been sorted, the next process is to find the number of slices and the number of directions of the DICOM file. A DICOM file with DWI (Diffusion Weighted Image) type used in this process is a scanning image in several different directions. After the files have been sorted, the next process is to rearrange the files according to the number of slices and the directions. This process is done by reading the metadata of image position patient index to Z. Image position patient metadata is generally obtained based on the value of the DICOM tag number (0020, 0032). However, on GE's scanning machine image position patient metadata is obtained based on the value of the DICOM tag number (0020, 9301). The value of Image Position Patient index to Z itself is the same for each slice in several different directions. Based on these characteristics, the number of slices can be determined by checking the number of different Image Position Patient values. If the number of slices has been obtained, the number of directions can be calculated by dividing the number of files by the number of slices.

The last process is to rearrange the DICOM files that have been sorted according to the number of slices and directions. One example is if there are 480 DICOM files with information on the number of slices is 30 and the number of directions is 16. Then we can change the value of 480 to 30 x 16.

B. Extraction of B-Value and B-Vector

B-Value is the weight value in the DWI image type. B-Vector is the gradient value in DWI image type. The B-Value and B-Vector on the DICOM files can be retrieved based on metadata values. The values of B-Value and B-Vector will be the same at different slices for the same time in one direction. However, the DICOM tag numbers that are used may vary, it depends on the type of scanning machine that is used to get the files. In this research, we used the scanning machine of GE Healthcare Company. This B-Value and B-Vector will be used to calculate the value of the B-Matrix. The B-Matrix will be used in the FA calculation process later. Table I is a detailed

DICOM tag for retrieving B-Value and B-Vector values from each vendor's scanning machine.

TABLE I. DICOM TAGS FOR EACH TYPE OF SCANNING MACHINE

DICOM Tag	Scanning Machine	Notes
(0018, 9087)	Common / Philips	B-Value
(0018, 9076)	Common / Philips	B-Vector (X, Y, Z)
(0019, 100C)	SIEMENS	B-Value
(0019, 100E)	SIEMENS	B-Vector (X, Y, Z)
(0065, 1009)	UIH	B-Value
(0065, 1037)	UIH	B-Vector (X, Y, Z)
(2001, 1003)	Old Philips	B-Value
(2005, 10B0)	Old Philips	B-Vector (X)
(2005, 10B1)	Old Philips	B-Vector (Y)
(2005, 10B2)	Old Philips	B-Vector (Z)
(0043, 1039)	GE	B-Value
(0019, 10BB)	GE	B-Vector (X)
(0019, 10BC)	GE	B-Vector (Y)
(0019, 10BD)	GE	B-Vector (Z)
(0018, 9087)	CANON	B-Value
(0020, 4000)	CANON	B-Vector (X,Y,Z)
(0018, 9087)	Bruker	B-Value
(0177, 1100)	Bruker	B-Vector (X,Y,Z)

C. Interpolate the number of slices in each direction

The interpolation process is used to improve image quality when viewed from other directions. Interpolation is a relatively easy approach to dealing with problems where we need information that is not explicitly available on existing data. For example, if the picture is taken from the Axial direction with a size of 256 x 256 and the number of slices is 30. So, if we look at the picture from the direction of Sagittal and Coronal will look less good. This is because the range value of the image resolution with the number of slices is too far away. Therefore, it is necessary to improve the number of slices. The interpolation process used is linear interpolation in the direction of Axial. The interpolation process is done based on Equation (1).

$$y = \frac{y_0(x_1 - x) + y_1(x - x_0)}{x_1 - x_0} \quad (1)$$

Based on Equation (1) y is the value of each pixel of the image to be interpolated. x_1 is the coordinate of the image at the upper limit. x is the coordinate of the image to be interpolated. x_0 is the coordinate of the image on the lower limit. y_0 is the value of each pixel of the image at the lower limit, and y_1 is the value of each pixel of the image at the upper limit.

Before we interpolate the number of slices, we must determine the target number of interpolation first. The target amount of interpolation can be obtained based on the calculation ratio between voxel spacing and pixel value. Assume that T_z is the target number of interpolations, P_z is the current number of slices, P_x is the size of pixel index to x, W_x is voxel spacing index to x, and W_z is voxel spacing index to z. Based on these variables, we can create an Equation to calculate the target interpolation described in Equation (2).

$$T_z = \frac{(P_z W_z) P_x}{P_x W_x} \quad (2)$$

In the DICOM data, the target number of slices to be interpolated is obtained based on the ratio of the current image size and the number of slices that exist in the value of pixel spacing and slice thickness metadata. Pixel spacing metadata is retrieved based on the value of the DICOM tag number (0028, 0030), while slice thickness metadata is taken based on the value of the DICOM tag number (0018, 0050). The minimum coordinate of the slice is currently obtained based on the minimum value of the image position patient metadata. The maximum coordinate of the slice is currently obtained based on the maximum value of the Image Position Patient metadata.

D. Fractional Anisotropy

The first step in the process of calculating diffusion tensor is to calculate the value of diffusion tensor matrix notation, or in this study, we refer to as B-Matrix $BMat$. B-Matrix is calculated based on the values of B-Value and B-Vector in each direction. B-Matrix is a matrix consisting of six main values ($BMat_{xx}$, $BMat_{yy}$, $BMat_{zz}$, $BMat_{xy}$, $BMat_{xz}$, $BMat_{zz}$). If we describe it in the form of a matrix, a 3x3 matrix will be formed. B-Matrix structure can be seen in Equation (3).

$$BMat = \begin{bmatrix} BMat_{xx} & BMat_{xy} & BMat_{xz} \\ BMat_{yx} & BMat_{yy} & BMat_{yz} \\ BMat_{zx} & BMat_{zy} & BMat_{zz} \end{bmatrix} \quad (3)$$

Based on Equation (3), the value of the B-Matrix is symmetrical ($BMat_{xy} = BMat_{yx}, BMat_{xz} = BMat_{zx}$, $BMat_{yz} = BMat_{zy}$). The value of the B-Matrix for each direction can be calculated based on Equation (4).

$$BMat = [-(BVal)(Bvec_x Bvec_x) - (BVal)(Bvec_y Bvec_y) - (BVal)(Bvec_z Bvec_z) - 2(BVal)(Bvec_x Bvec_y) - 2(BVal)(Bvec_x Bvec_z) - 2(BVal)(Bvec_y Bvec_z)] \quad (4)$$

Based on Equation (4), $BVal$ is the value of the B-Value. $Bvec_x$, $Bvec_y$, and $Bvec_z$ are the values of the B-Vector in each index, namely: index x, y, and z. When the value of the diffusion tensor or B-Matrix is known, the next process is to calculate the value of the diffusion tensor image. The calculation of diffusion tensor image value is done on each voxel.

Before entering into the anisotropy calculation of the diffusion tensor, the eigenvalue and eigenvector values of each voxel must be calculated first [25]. The three eigenvalue values obtained $(\lambda_1, \lambda_2, \lambda_3)$ are values that will define the ellipsoid diffusion shape. While the three eigenvector values obtained (v_1, v_2, v_3) will define the orientation of the ellipsoid diffusion [26]. After we got those six values, the next process is to calculate the value of the anisotropy diffusion tensor [27]. At this time, the widely used method of anisotropy calculation is fractional anisotropy. FA is a method measured using diffusion tensor imaging [28]. This method of anisotropy

calculation is described by Basser and Piarpaoli [29]. The Equation for calculating FA values is described in Equation (5).

$$FA = \sqrt{\frac{((\lambda_1 - \lambda_2)^2 + (\lambda_2 - \lambda_3)^2 + (\lambda_3 - \lambda_1)^2)}{2(\lambda_1^2 + \lambda_2^2 + \lambda_3^2)}} \quad (5)$$

Based on Equation (5), λ_1, λ_2, and λ_3 are the eigenvalues used to calculate the FA value. This FA process will determine the position as well as the direction of the diffusion. There are only six unknowns ($D_{xx}, D_{yy}, D_{zz}, D_{xy}, D_{xz}, D_{zz}$) in the diffusion tensor matrix notation. Thus if we have six-directional DW data set then the unknown diffusion constants can be obtained by solving the Equation. In this FA process, the shape used is an ellipsoid because it can determine the direction of diffusion.

E. Fiber Tracking

The fiber tracking process is carried out from the FA data that has been obtained previously. The fiber tracking process usually also depends on the eigenvector value that has been calculated previously on each voxel [30].

IV. Result and Discussion

The experiment was conducted using 6 datasets. We divide this dataset into 2 types. The first type of dataset is the internal dataset, this data we obtained from hospitals and not used for the public. The second type of dataset is an external dataset, this data we obtained from one of the webs that provides an open-source data. The dataset used are not divided into training data and testing data. All datasets will be directly do the fiber extraction process using the same method.

The dataset used consists of several different types of scanning machines. Dataset 1 consists of 480 DICOM files. Dataset 2 consists of 4344 DICOM files. Dataset 3 consists of 1628 DICOM files. Dataset 4 consists of 2380 DICOM files. Dataset 5 consists of 2380 DICOM files. Dataset 6 consists of 31 DICOM files. Datasets 1 and 2 are datasets obtained from the National Hospital, Surabaya. Datasets 3, 4, 5, and 6 are external datasets obtained from the Aliza Medical Imaging website. Datasets 1, 2, and 3 are obtained using GE-type scan machines. Datasets 4 and 5 are obtained using Philips-type scan machines. Dataset 6 was obtained using the Siemens type scan machine.

As a comparison, we will use NIfTI data for constructing 3D DTI as many previous studies have done. The results of the 3D DTI will be compared visually and the number of neural fibers that have been successfully extracted. The neural fibers to be extracted are neural fibers with a minimum length of 50 mm and a maximum length of 600 mm. The results of the fiber tracking on all datasets are shown in Table II. Detail amounts of fibers in each dataset are shown in Table III.

Based on Table II, the results of the fiber tracking process using our approach that used DICOM data directly show better visually. This can be seen from the density of the neural fibers formed. In addition, the amounts of neural fibers formed are also greater. This is evidenced by the values shown in Table III.

TABLE II. Fiber Tracking Result

Dataset	Fiber Tracking Result	
	Proposed Method	***NIfTI***
1	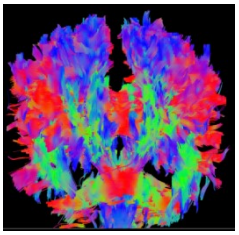	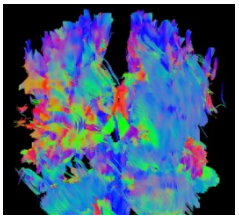
2	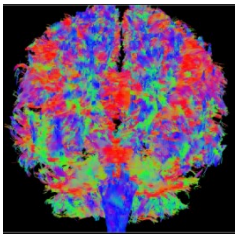	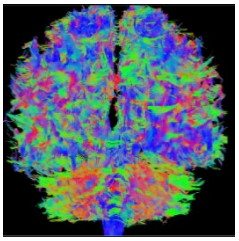
3	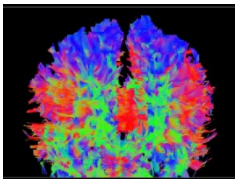	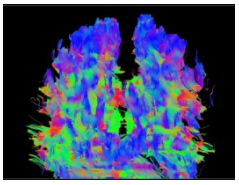
4	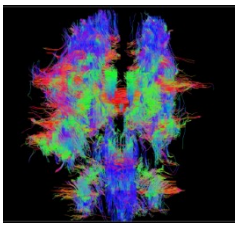	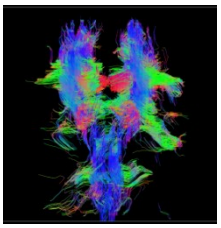
5	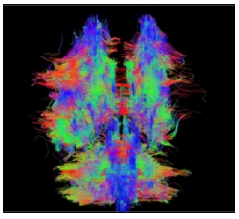	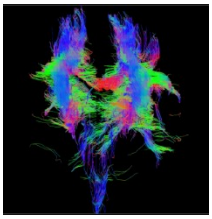
6	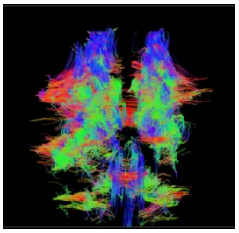	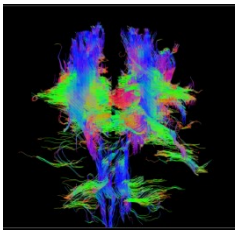

TABLE III. DETAILS NUMBER OF FIBERS

Dataset	Detail Amounts of Fibers	
	Proposed Method	*NIfTI*
1	**316412**	240948
2	**318533**	252753
3	**247974**	186040
4	**16920**	6404
5	**17920**	7082
6	**15448**	8943
Average	**155534.5**	117028.3

Based on Table III, number 1 is the result of fiber tracking process using the GE scan machine. In number 1, our approach produces better 3D images with an increase in the amount of fiber by 75464 or about 31%. Number 2 is the result of the fiber tracking process using the GE scan machine. In number 2, our approach produces an increase in the amount of fiber by 65780 or about 26%. Number 3 is the result of the fiber tracking process using the GE scan machine. In number 3, our approach produces an increase in the amount of fiber by 61934 or about 33%. Number 4 is the result of the fiber tracking process using the Philips scan machine. In number 4, our approach produces an increase in the amount of fiber as much as 10516 or about 164%. Number 5 is the result of the fiber tracking process using the Philips scan machine. In number 5, our approach produces an increase in the amount of fiber by 10838 or about 153%. Number 6 is the result of the fiber tracking process using a Siemens scan machine. In number 6, our approach produces an increase in the amount of fiber by 6505 or about 72%.

There is an increase in the results of all the datasets that used in this study. On average, there was an increase in the amounts of neural fibers formed around 38606, or about 32.9% of the six datasets used in this study. The more or denser the neural fibers that was extracted, it means that the more complete the neural fibers that was produced. This higher number of neural fibers corresponds to the visualization of fiber shapes in Table II. Visualization of fiber shapes in the proposed method that utilizes DICOM data directly has a denser neural shape.

With the more complete of the neural fibers, it is more useful for the doctor to see the details of the neural fibers in a particular part of the brain anatomy. So that if there is an abnormality in the brain, the doctor can see how the neural fibers in it is better.

V. CONCLUSION

In this study, we proposed an approach for constructing 3D DTI using DICOM data directly and a linear interpolation method to improve the neural fibers extraction results. We use the DICOM data directly because DICOM data stores a lot of information that can be used for further research. Direct use of DICOM data is also used to maximize neural fibers extraction results. We also compared the proposed method with the use of NIfTI data that is widely used by recent studies.

Based on the experiment results, our approach has been proven to improve the quality of neural fibers extraction results. We can see it based on the amount of fiber that has been formed. Our approach produces an average amount of neural fibers around 155534 fibers, while when we use NIfTI data are about 117028 fibers. The difference in fibers around 38606 or an increase about 32.9% is enough to prove that the use of DICOM data directly can provide better neural fibers extraction results. The direct use of DICOM data also has the advantage that the information of each DICOM file is still stored properly and can be used for further 3D image processing, like segmentation or registration.

The following research will carry out further processing on the 3D DTI images that have been formed. Processing that will be carried out includes registration of 3D DTI images with other types of medical images to assist doctors in planning better surgical procedures. As well as segmenting some brain anatomy to analyze the structure of the brain's neural network in certain anatomy.

ACKNOWLEDGMENT

This research was funded by Lembaga Pengelola Dana Pendidikan (LPDP) under Riset Inovatif-Produktif (RISPRO) Invitation Program, the Indonesian Ministry of Education and Culture under Penelitian Terapan Unggulan Perguruan Tinggi (PTUPT) Program, and Institut Teknologi Sepuluh Nopember (ITS) under project scheme of the Publication Writing and Intellectual Property Rights Incentive Program (PPHKI)

REFERENCES

[1] P. Damayanti, D. Yuniasri, R. Sarno, A. Fajar, and D. Rahmawati, "Corpus Callosum Segmentation from Brain MRI Images Based on Level Set Method," *Int. Semin. Appl. Technol. Inf. Commun.*, 2020.

[2] A. Fajar, R. Sarno, C. Fatichah, and A. Fahmi, "Reconstructing and resizing 3D images from DICOM files," *J. King Saud Univ. - Comput. Inf. Sci.*, 2021, doi: 10.1016/j.jksuci.2020.12.004.

[3] A. S. Nugroho, A. Fajar, R. Sarno, C. Fatichah, A. Fahmi, S. A. Utomo, and F. Notopuro, "Unsupervised Method for 3D Brain Magnetic Resonance Image Segmentation," *Proc. - 2021 IEEE Asia Pacific Conf. Wirel. Mobile, APWiMob 2021*, pp. 90–94, 2021, doi: 10.1109/APWiMob51111.2021.9435267.

[4] E. K. Susanto, Junaidi, F. A. Hizham, R. Sarno, and A. Fajar, "Unsupervised Corpus Callosum Extraction for T2-FLAIR MRI Images," *3rd 2021 East Indones. Conf. Comput. Inf. Technol. EIConCIT 2021*, pp. 116–121, 2021, doi: 10.1109/EIConCIT50028.2021.9431894.

[5] L. Atikah, N. A. Hasanah, R. Sarno, A. Fajar, and D. Rahmawati, "Brain segmentation using adaptive thresholding, k-means clustering and mathematical morphology in MRI Data," *Proc. - 2020 Int. Semin. Appl. Technol. Inf. Commun. IT Challenges Sustain. Scalability, Secur. Age Digit. Disruption, iSemantic 2020*, pp. 161–167, 2020, doi: 10.1109/iSemantic50169.2020.9234303.

[6] H. Bao, R. Li, M. He, D. Kang, and L. Zhao, "DTI Study on Brain Structure and Cognitive Function in Patients with Chronic Mountain Sickness," *Sci. Rep.*, 2019, doi: 10.1038/s41598-019-55498-9.

[7] R. E. Sondergaard, C. P. Rockel, F. Cortese, Y. Jasaui, T. M. Pringsheim, J. R. Sarna, O. Monchi, A. F. Sadikot, B. G. Pike, and D. Martino, "Microstructural Abnormalities of the Dentatorubrothalamic Tract in Cervical Dystonia," *Mov. Disord.*, vol. 36, no. 9, pp. 2192–2198, 2021, doi: 10.1002/mds.28649.

[8] S. Lijdsman, M. Königs, M. S. van Sandwijk, A. H. Bouts, K. van Hoeck, H. de Jong, M. Engelen, J. Oosterlaan, F. J. Bemelman, K. J. Oostrom, and J. W. Groothof, "Structural brain abnormalities in children and young adults with severe chronic kidney disease,"

Pediatr. Nephrol., no. 0123456789, 2021, doi: 10.1007/s00467-021-05276-5.

[9] P. Adamczyk, O. Płonka, D. Kruk, M. Jáni, P. Błądziński, A. Kalisz, S. Castelein, A. Cechnicki, and M. Wyczesany, "On the relation of white matter brain abnormalities and the asociality symptoms in schizophrenia outpatients – a dti study," *Acta Neurobiol. Exp. (Wars).*, vol. 81, no. 1, pp. 80–95, 2021, doi: 10.21307/ane-2021-009.

[10] P. Nigro, A. Chiappiniello, S. Simoni, F. P. Paoletti, G. Cappelletti, P. Chiarini, M. Filidei, P. Eusebi, G. Guercini, V. Santangelo, R. Tarducci, P. Calabresi, L. Parnetti, and N. Tambasco, "Changes of olfactory tract in Parkinson's disease: a DTI tractography study," *Neuroradiology*, vol. 63, no. 2, pp. 235–242, 2021, doi: 10.1007/s00234-020-02551-4.

[11] M. Bergamino, E. G. Keeling, R. R. Walsh, and A. M. Stokes, "Systematic assessment of the impact of DTI methodology on fractional anisotropy measures in Alzheimer's disease," *Tomography*, vol. 7, no. 1, pp. 20–38, 2021, doi: 10.3390/tomography7010003.

[12] J. Yang, Y. Wang, and L. Wang, "Topological Characteristics Associated with Intraoperative Stimulation Related Epilepsy of Glioma Patients : A DTI Network Study," pp. 1–17, 2021.

[13] S. U. Sadat, H. H. Shomee, A. Awwal, S. N. Amin, and T. Reza, "Alzheimer ' s Disease Detection and Classification using Transfer Learning Technique and Ensemble on Convolutional Neural Networks," no. January, pp. 17–20, 2021.

[14] Y. Shirazi, M. A. Oghabian, and S. A. H. Batouli, "Along-tract analysis of the white matter is more informative about brain ageing, compared to whole-tract analysis," *Clin. Neurol. Neurosurg.*, vol. 211, no. 88, p. 107048, 2021, doi: 10.1016/j.clineuro.2021.107048.

[15] J. Pan, B. Lei, S. Wang, B. Wang, Y. Liu, and Y. Shen, "DecGAN: Decoupling Generative Adversarial Network detecting abnormal neural circuits for Alzheimer's disease," pp. 1–11, 2021, [Online]. Available: http://arxiv.org/abs/2110.05712.

[16] X. Xia, L. Dai, H. Zhou, P. Chen, S. Liu, W. Yang, Z. Zuo, and X. Xu, "Assessment of peripheral neuropathy in type 2 diabetes by diffusion tensor imaging: A case-control study," *Eur. J. Radiol.*, vol. 145, no. September, p. 110007, 2021, doi: 10.1016/j.ejrad.2021.110007.

[17] J. Moona, P. Bremer, P. Mukherjee, A. J. Markowitz, E. M. Palaciosb, A. Rodriguez, Y. Xiao, G. T. Manley, and R. K. Madduric, "MaPPeRTrac: A Massively Parallel, Portable, and Reproducible Tractography Pipeline," 2020.

[18] J. Hodel, J. P Lefaucheur, S. Tolédano, N. Badat, C. Rondenet, M. Zuber, M. Zins, and A. Créange, "Diffusion tensor imaging MR neurography in patients with acute or chronic plexopathy," *J. Neuroradiol.*, vol. 000, 2021, doi: 10.1016/j.neurad.2021.06.002.

[19] E. Leroux, A. Vandevelde, M. Tréhout, and S. Dollfus, "Abnormalities of fronto-subcortical pathways in schizophrenia and the differential impacts of antipsychotic treatment: a DTI-based tractography study," *Psychiatry Res. - Neuroimaging*, vol. 280, no. February, pp. 22–29, 2018, doi: 10.1016/j.pscychresns.2018.08.008.

[20] L. C. Liebrand, G. A. van Wingen, F. M. Vos, D. Denys, and M. W. A. Caan, "Spatial versus angular resolution for tractography-assisted planning of deep brain stimulation," *NeuroImage Clin.*, vol. 25, p. 102116, 2020, doi: 10.1016/j.nicl.2019.102116.

[21] V. A. Coenen, B. Sajonz, M. Reisert, J. Bostroem, B. Bewernick, H. Urbach, C. Jenkner, P. C. Reinacher, T. E. Schlaepfer, and B. Mädler, "Tractography-assisted deep brain stimulation of the superolateral branch of the medial forebrain bundle (slMFB DBS) in major depression," *NeuroImage Clin.*, vol. 20, pp. 580–593, 2018, doi: 10.1016/j.nicl.2018.08.020.

[22] G. E. Umana, G. Scalia, F. Graziano, R. Maugeri, N. Alberio, F. Barone, A. Crea, S. Fagone, G. R. Giammalva, L. Brunasso, R. Costanzo, F. Paolini, R. M. Gerardi, S. Tumbiolo, S. Cicero, G. F. Nicoletti, and D. G. Iacopino, "Navigated transcranial magnetic stimulation motor mapping usefulness in the surgical management of patients affected by brain tumors in eloquent areas: A systematic review and meta-analysis," *Front. Neurol.*, vol. 12, no. March, pp. 1–8, 2021, doi: 10.3389/fneur.2021.644198.

[23] V. A. Coenen, C. Jenkner, C. R. Honey, and B. Mädler, "Electrophysiologic validation of diffusion tensor imaging tractography during deep brain stimulation surgery," *Am. J. Neuroradiol.*, vol. 37, no. 8, pp. 1470–1478, 2016, doi: 10.3174/ajnr.A4753.

[24] J. E. Reynolds, X. Long, D. Paniukov, M. Bagshawe, and C. Lebel, "Calgary Preschool magnetic resonance imaging (MRI) dataset," *Data Br.*, 2020, doi: 10.1016/j.dib.2020.105224.

[25] P. C. Sundgren, Q. Dong, D. Gómez-Hassan, S. K. Mukherji, P. Maly, and R. Welsh, "Diffusion tensor imaging of the brain: Review of clinical applications," *Neuroradiology*, vol. 46, no. 5, pp. 339–350, 2004, doi: 10.1007/s00234-003-1114-x.

[26] T. Moritani, S. Ekholm, P.-L. Westesson, and J. Zhong, "Basics of Diffusion Measurements by MRI," *Diffus. MR Imaging Brain*, pp. 1–5, 2009, doi: 10.1007/978-3-540-78785-3_1.

[27] P. S. Hüppi and J. Dubois, "Diffusion tensor imaging of brain development," *Semin. Fetal Neonatal Med.*, vol. 11, no. 6, pp. 489–497, 2006, doi: 10.1016/j.siny.2006.07.006.

[28] P. Kochunov, D. E. Williamson, J. Lancaster, P. Fox, J. Cornell, J. Blangero, and D. C. Glahn, "Fractional anisotropy of water diffusion in cerebral white matter across the lifespan," *Neurobiol. Aging*, vol. 33, no. 1, pp. 9–20, 2012, doi: 10.1016/j.neurobiolaging.2010.01.014.

[29] C. G. Koay, L. C. Chang, J. D. Carew, C. Pierpaoli, and P. J. Basser, "A unifying theoretical and algorithmic framework for least squares methods of estimation in diffusion tensor imaging," *J. Magn. Reson.*, vol. 182, no. 1, pp. 115–125, 2006, doi: 10.1016/j.jmr.2006.06.020.

[30] P. Mukherjee, S. W. Chung, J. I. Berman, C. P. Hess, and R. G. Henry, "Diffusion tensor MR imaging and fiber tractography: Technical considerations," *Am. J. Neuroradiol.*, vol. 29, no. 5, pp. 843–852, 2008, doi: 10.3174/ajnr.A1052.